

Ionic Components of Wound Current at Mouse Skin Incisional Wounds

Zhongren Sun^{1, 2*}, Jinhuan Yue^{1, 2*} and Qinhong Zhang^{2,3}

¹Neurobiology Laboratory of Acupuncture and moxibustion, Heilongjiang University of Chinese Medicine, Harbin, 150040, China.

²Department of Acupuncture and Moxibustion, Second Affiliated Hospital of Heilongjiang University of Chinese Medicine, Harbin, 150040, China.

³Department of Health Research and Policy, Stanford University, CA, 94305, USA.

Abstract: It has been assumed that skin wound currents are produced by passive ion leakage from wounded skin. However, what ions contribute to the skin wound current? Thirty male C57BL/6 mice were used in this study. A lancet wound (about 5mm in length) was made by cutting into the full thickness skin. We measured the dynamic time courses of individual ion flux with ion-selective probes at skin wound. The probe is aligned perpendicular to the surface of skin wound. All ions (Na⁺, Cl⁻, K⁺, Ca²⁺ and H⁺) showed a small steady efflux at unwounded mouse skin. However, there were large efflux of Na⁺, Cl⁻, K⁺, Ca²⁺ and H⁺ 15 minutes after wounding. These values maintained for 534 seconds, which were significantly higher than the ions flux of intact skin ($P < 0.05$). Our results suggest that Na⁺, Cl⁻, K⁺, Ca²⁺ and H⁺ contribute to the wound currents at skin wounds. A most significant observation is that the skin wound currents are carried mainly by the largest sodium and chloride efflux, then potassium, while the calcium and hydrogen are the least.

Key words: Skin wound; wound healing; wound current; ion fluxes; sodium flux; chloride flux; potassium flux; calcium flux; hydrogen flux.

Introduction

Endogenous wound electric fields were first identified more than 150 years ago by the German physiologist Emil Du-Bois Reymond (1). Such electric fields are generated when the epithelial layer is disrupted instantaneously and the lesion short-circuits the transepithelial potential difference (2-7). Electric currents at wounds in human skin (4, 8-11) and in rodent cornea and skin (5, 7, 12-13) have been measured with various techniques, such as vibrating probes, micro-glass electrodes, micro-needle arrays, and bioelectric imagers (5, 12, 14-16). For example, it is reported that a large outward current of 4 mA cm⁻² was measured at the wound edges of rat cornea and human skin. This current gradually increased to 10 mA cm⁻² and persisted at 4-8 mA cm⁻² (17).

Electric signals play a critical role in cell migration during wound healing (5, 17-18). It has been shown that exogenous fields directs many types of cells to divide, migrate and differentiate in the process of electrotaxis, a phenomenon that many types of cells respond to applied electric fields by directional cell migration, such as skin epithelial cells (19), corneal epithelial cells (20-23), keratinocytes (24-25), fibroblasts (26) and neuronal cells (27-29).

It has been confirmed that consistent and sustained outward electric currents are found at wounds in human skin and in rodent cornea and skin (4-5, 7-13). Our own and other studies have shown that ions fluxes (Na⁺, Cl⁻, K⁺, Ca²⁺, H⁺) contribute to the wound currents. However, the wound currents from different tissues result from different

major ions fluxes. For example, Cl⁻ mainly contributes to rat cornea wound currents (30). However, what about the skin wound currents? In this study, we will find out what kinds of ions fluxes contribute to the skin wound current.

Materials and Methods

Materials

All ions fluxes (Na⁺, Cl⁻, K⁺, Ca²⁺ and H⁺) were measured noninvasively using SIET (SIET system BIO-001A; Younger USA Sci. & Tech. Corp.; Applicable Electronics Inc.; and ScienceWares Inc.) at the Xu-Yue company (Sci. & Tech. Co. Ltd, Beijing, China; <http://www.xuyue.net>). Electrodes were calibrated in Ionophore Cocktails A (K⁺(0.3 mM), Cl⁻(0.3 mM), Na⁺(0.4 mM), Ca²⁺(0.05 mM)) (containing 0.1 mM KCl, 0.05 mM CaCl₂, 0.1mM NaCl, 0.1 mM KH₂PO₄, 0.1 mM NaHCO₃, 0.1 mM Na₂HPO₄, 5.6 mM Glucose, pH7.2) and Ionophore Cocktails B (K⁺(3.2 mM), Cl⁻(14 mM), Na⁺(10.3 mM), Ca²⁺(0.5 mM)) (containing 3 mM KCl, 0.5 mM CaCl₂, 10mM NaCl, 0.1 mM KH₂PO₄, 0.1 mM NaHCO₃, 0.1 mM Na₂HPO₄, 5.6 mM Glucose, pH7.2). The H⁺ was also calibrated in the same Ionophore Cocktails A and Ionophore Cocktails B, but pH was adjusted from 7.2 to 7.6 and from 7.2 to 6.7 respectively. The tips of the ion-selective microelectrodes used to measure the ions fluxes of skin wound mouse were dipped in the test solution (K⁺(0.6 mM), Cl⁻(1.7 mM), Na⁺(1.3 mM), Ca²⁺(0.1 mM)) (containing 0.5 mM KCl, 0.1 mM CaCl₂, 1mM NaCl, 0.1 mM KH₂PO₄, 0.1 mM NaHCO₃, 0.1 mM Na₂HPO₄, 5.6 mM Glucose, pH7.2).

Table 1. The basic information of electrodes.

Name	Catalog number	Source	Used for tissue
Na ⁺	Φ5±1 μm, XY-DJ-01	YoungerUSA	skin
Cl ⁻	Φ9±1 μm, XY-DJ01	YoungerUSA	skin
K ⁺	Φ5±1 μm, XY-DJ-01	YoungerUSA	skin
Ca ²⁺	Φ5±1 μm, XY-DJ-01	YoungerUSA	skin
H ⁺	Φ5±1 μm, XY-DJ-01	YoungerUSA	skin

Preparation of the ion selective microelectrodes

Take Cl⁻-selective microelectrodes for example, the preparation of ion selective microelectrodes was described as follows: first, pre-pulled and silanized glass micro-pipettes (Φ9±1 μm, XY-DJ01, YoungerUSA (YoungerUSA LLC, Amherst, MA 01002, USA), Table 1) were first filled with a backfilling solution (100 mM KCl, Table 2) to a length of approximately 1.0 cm from the tip. The micro-pipettes were front filled with 15-50 μm columns of selective liquid ion-exchange cocktails (Cl⁻ LIX, XY-SJ-Na, YoungerUSA, Table 2). An Ag/AgCl wire electrode holder (XY-DJGD, YoungerUSA) was inserted in the back of the electrode to make electrical contact with the electrolyte solution. YG003-Y05 (YoungerUSA) was used as the reference electrode.

Calibration of the ion selective microelectrodes

Prior to the flux measurement, the microelectrodes were calibrated with cultural media having different concentrations of Cl⁻, 1.7 mM and 0.3 mM respectively. Only electrodes with Nernst slope < -53 mV/decade were used in our study (Table 2). The same microelectrodes were calibrated again according to the same procedure and standards after each test. Data was discarded if the post-test calibrations failed. The microelectrode moved repeatedly from one point to another perpendicular to the surfaces of skin at a frequency of cl. 0.3Hz. Moreover, the distance between two points is usually between 5 to 35 μm, and we used 30 μm throughout the experiments.

Animals & Wound Model

Thirty male C57BL/6 mice (18-22g) were used in this study. All mice were housed according to the National guidelines for the care and use of laboratory animals. All protocols were approved by the Institutional Animal Care and Use Committee of the Heilongjiang University of Chinese Medicine. Mice were anaesthetised by intraperi-toneal administration of pentobarbital sodium (60 mg/kg)

Table 2. The related parameters of various LIX.

Name	Catalog number	Source	Sigma batch	CS-LIX-C	Backfilling solution	Nernst Slope (mV/decade)
Na ⁺	XY-SJ-Na	YoungerUSA	#71178	15-50 μm	250 mM NaCl	> 53
Cl ⁻	XY-SJ-Cl	YoungerUSA	#24902	15-50 μm	100 mM KCl	< -53
K ⁺	XY-SJ-K	YoungerUSA	#60031	180 μm	100 mM KCl	> 53
Ca ²⁺	XY-SJ-Ca	YoungerUSA	#21048	15-50 μm	100 mM CaCl	> 26
H ⁺	XY-SJ-H	YoungerUSA	#95293	15-50 μm	15 mM NaCl +40 mM KH ₂ PO ₄ , pH 7.0	> 53

Note: LIX: liquid ion exchangers; CS-LIX-C: columns of selective LIX cocktails.

before the measurement. Hair from the back was shaved and then the area was antisepticed with VEET Cream. We made a lancet wound (about 5mm in length) by cutting into the full thickness skin, one wound on each mouse, six mice for each ion flux (11).

Measurement of ionic flux at skin wounds

We access the different regions of the skin wound to find out the largest ion flux. Take Cl⁻ flux for an example, we move the probe to a reference position near the wound edge and start recording a baseline. When a stable baseline has been established, move the probe to the measuring po-sition. The probe is aligned perpendicular to the surface of skin wound. The distance from among the different measuring positions is about 300 μm. Observe the trace until it becomes stable, and stop measuring when it falls back to baseline.

Statistical analysis

Data were analyzed using Microsoft Excel and results are expressed as mean ± standard error (SE). Statistical significance was assessed using Student's *t* test and *P* <0.05 was considered statistically significant difference.

Results

We present the data from ion-selective measurement as ion flux, calculated and recorded data with the probe in self-referencing mode close to the wound center.

We first measured Na⁺ flux at unwounded mouse skin, and it showed a slightly efflux. However, a larger efflux of Na⁺ of 24.37 nmol cm⁻² s⁻¹ was tested at skin wound center 15 minutes after skin wounded (*P* < 0.01), this value was maintained for 534 seconds (Figure 1).

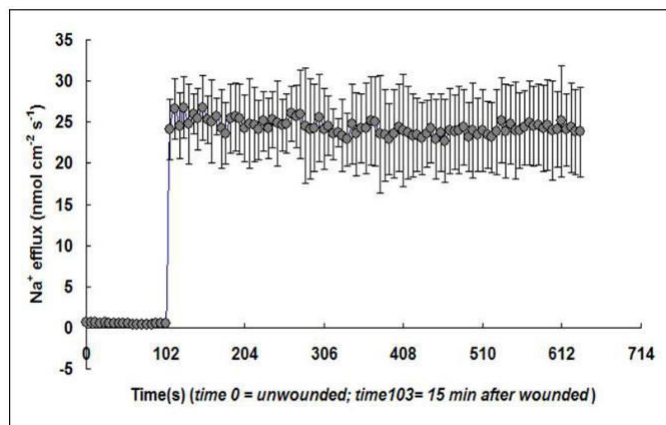


Figure 1. Sodium flux at skin wounds.

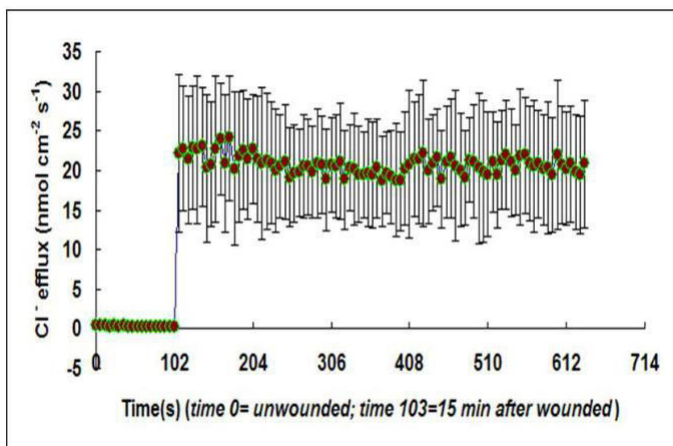


Figure 2. Chloride flux at skin wounds.

We then determined Cl⁻ flux. We saw a small chloride efflux in unwounded mouse skin. Fifteen minutes after wounding, it reached to larger efflux and sustained an average value of 20.70 nmol cm⁻² s⁻¹, that was significantly greater than unwounded flux (*P* < 0.01) (Figure 2).

Potassium efflux at unwounded mouse skin was slightly above the background. However, there was a rapid and large increase of potassium efflux at skin wound center from 0.43 nmol cm⁻² s⁻¹ to 4.41 nmol cm⁻² s⁻¹ 15 minutes after skin wounded (Figure 3). This high level of potassium efflux then dropped slowly, reaching a lower, stable value at 3.19 nmol cm⁻² s⁻¹ from 103-636 seconds after wounding which remained significantly higher than unwounded values (*P* < 0.01) (Figure 3).

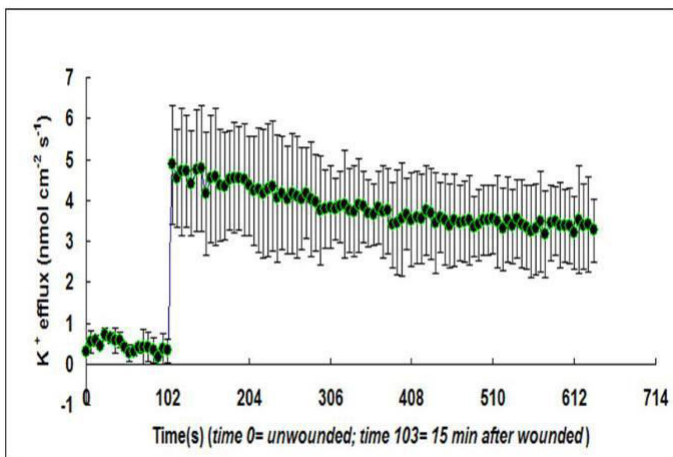


Figure 3. Potassium flux at skin wounds.

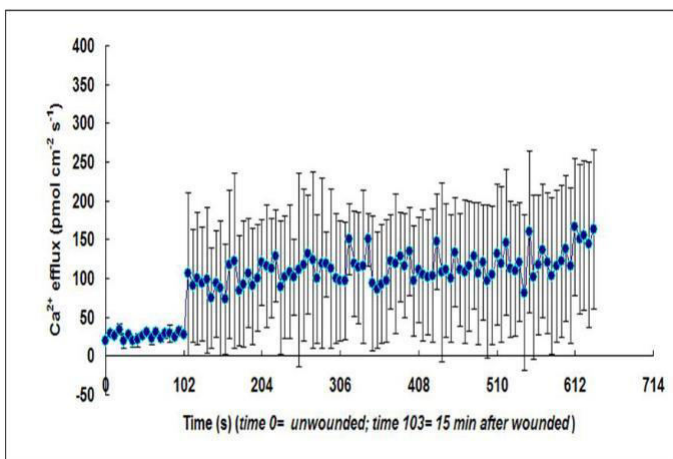


Figure 4. Calcium flux at skin wounds.

Intact skin showed a small efflux of calcium ions of 26.00 pmol cm⁻² s⁻¹. This value immediately reached up to 105.65 pmol cm⁻² s⁻¹ 15 minutes after skin wounded (*P* < 0.01) (Figure 4). This large efflux of Ca²⁺ still increased slowly to 160.46 pmol cm⁻² s⁻¹ with an average value of 113.1436 pmol cm⁻² s⁻¹ from 103-636 seconds, which is still significantly higher than unwounded values (*P* < 0.01) (Figure 4).

We found a small efflux of protons of 0.46 pmol cm⁻² s⁻¹ at unwounded mouse skins. The H⁺ efflux changes significantly up to 1.013297 pmol cm⁻² s⁻¹ 15 minutes after wounding. This value increased upon to 1.83 pmol cm⁻² s⁻¹ 20.2 minutes after wounding, and maintained for 222 seconds with average value of 1.59 pmol cm⁻² s⁻¹, which is significantly higher than the unwounded value (*P* < 0.05) (Figure 5).

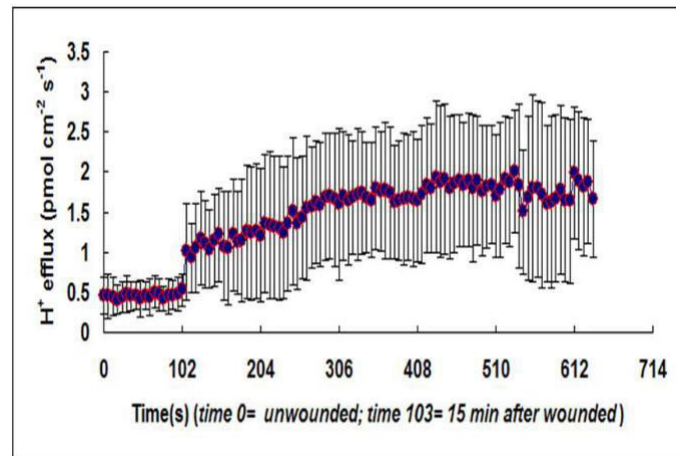


Figure 5. Hydrogen flux at skin wounds.

Comparing the relative contributions of different ion fluxes to the skin wound current showed an overriding contribution of Na⁺ and Cl⁻, then partly contributions of K⁺, and negligible of Ca²⁺ or H⁺ (Figure 6). We chose 537 seconds time point to collect data of the efflux of five ions. Thus, Na⁺ and Cl⁻ contribute to mouse skin wound mainly.

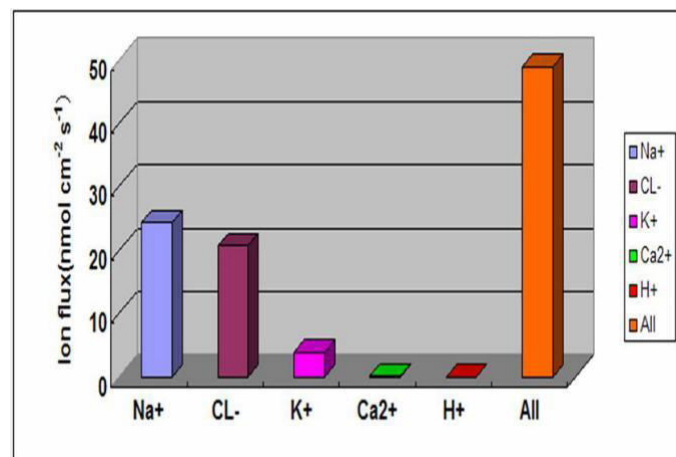


Figure 6. Relative contributions of ions to mouse skin wound current.

Discussion

It has long been assumed that endogenous wound electric fields played a very important role in wound healing, because endogenous electric currents and cells generated from wounds, which responded to applied electrical signals during the period of wound healing (2, 5, 7, 11, 19,

31-38). Some experimental evidence showed that wound current was detected from skin wounds (1, 15, 39-40). However, we still do not know what kinds of ions fluxes contribute to the skin wound current.

In this study, we studied the ionic components of naturally-occurring wound current of mouse skin wound. We used noninvasive apparatus SLET to measure the concentration gradient of Na⁺, Cl⁻, K⁺, Ca²⁺ and H⁺ by selective vibrated microelectrodes; and repeated between two points in the predefined fashion. The ionic fluxes were calculated based on the Fick's law of diffusion. First, the microvolts differences of the measured ions were exported as raw data. Then, imported and converted them into net ionic fluxes by using the JCal V3.2.1 (a free MS Excel spreadsheet, youngerusa.com or ifluxes.com).

Our study find out that Na⁺ and Cl⁻ make the most contributions, then K⁺ contributes partly to skin wound current, while the Ca²⁺ and H⁺ make negligible contributions, which is different from the cornea wound current, mainly by a large influx of chloride ions, and in part by effluxes of calcium and potassium ions (30).

Previous study found out that chloride flux is essential flux in corneal epithelial cells in amphibians (41, 42). However, in this study, we found the largest sodium efflux, and then chloride efflux. This may suggest that sodium flux significantly contribute to the electric current at skin wounds.

We have measured large ions efflux at skin wounds, which had a dynamic time course with ion selective microelectrode measurements. For example, all ions (including Na⁺, Cl⁻, K⁺, Ca²⁺ and H⁺) efflux at wound center with stable value 15 minutes after wounding and the dynamic time courses lasted 537seconds, except K⁺ efflux dropped slowly and Ca²⁺ and H⁺ efflux increased slightly, which are still significantly higher than the unwounded value.

The results of this study suggest a very important aspect in skin wound healing. The dynamic changes of specific ion fluxes, such as Na⁺, Cl⁻, K⁺, Ca²⁺ and H⁺ after skin wound suggest that electrical signaling is an active response to skin wound and offers potential intervention for skin wound healing, especially for chronic wound, such as pressure ulcers (43-46).

In summary, sodium and chloride efflux form a significant portion of the skin wound current, and then partly consist of potassium, calcium and hydrogen ions with time courses. Further study can be dig based on this study.

Acknowledgments

This research was supported by the National Natural Science Foundation of China (No. 81303045), and Foundation of Heilongjiang University of Traditional Chinese Medicine (No. 201106; No.2012RCQ64; No.2012RCL01).

Conflict of interest

The authors declare that they have no conflict of interests.

References

Du Bois-Reymond E. Vorläufiger Abriss einer Untersuchung über den sogenannten Froschstrom und die electromotorischen Fische. *Ann Phy U Chem* 1843; **58**:1-30. Ionic Components of Wound Current at Incisional Wounds.

2. Barker AT, Jaffe LF, Venable JW Jr. The glabrous epidermis of cavies contains a powerful battery. *Am J Physiol* 1982; **242**:358-66.
3. Jaffe LF, Nuccitelli R. An ultrasensitive vibrating probe for measuring steady extracellular currents. *J Cell Biol* 1974; **63**: 614-28.
4. Borgens RB, Venable JW Jr, Jaffe LF. Bioelectricity and regeneration: large currents leave the stumps of regenerating newt limbs. *Proc Natl Acad Sci USA* 1977; **74**: 4528-32.
5. Reid B, Song B, McCaig CD, Zhao M. Wound healing in rat cornea: the role of electric currents. *FASEB J* 2005; **19**:379-86.
6. Keese CR, Wegener J, Walker SR, Giaever I. Electrical wound-healing assay for cells in vitro. *Proc Natl Acad Sci USA* 2004; **101**:1554-9.

7. Robinson KR, Messerli MA. Left/right, up/down: the role of endogenous electrical fields as directional signals in development, repair and invasion. *BioEssays* 2003; **25**:759-66.
8. Borgens RB, Venable JW Jr, Jaffe LF. Bioelectricity and regeneration. I. Initiation of frog limb regeneration by minute currents. *J Exp Zool* 1977; **200**:403-16.
9. Borgens RB, Venable JW Jr, Jaffe LF. Role of subdermal current shunts in the failure of frogs to regenerate. *J Exp Zool* 1979; **209**: 49-56.
10. Illingworth CM, Barker AT. Measurement of electrical currents emerging during the regeneration of amputated fingertips in children. *Clin Phys Physiol Meas* 1980; **1**: 87-9.
11. Guo A, Song B, Reid B, Gu Y, Forrester JV, Jahoda CA, Zhao M. Effects of physiological electric fields on migration of human dermal fibroblasts. *J Invest Dermatol* 2010; **130**(9):2320-7.
12. Chiang M, Robinson KR, Venable JW Jr. Electrical fields in the vicinity of epithelial wounds in the isolated bovine eye. *Exp Eye Res* 1992; **54**: 999-1003.
13. Wang E, Reid B, Lois N, Forrester JV, McCaig CD, Zhao M. Electrical inhibition of lens epithelial cell proliferation: an additional factor in secondary cataract? *FASEB J* 2005; **19**:842-4.
14. Mukerjee EV, Isseroff RR, Nuccitelli R, Collins SD, Smith RL. Microneedle array for measuring wound generated electric fields. *Conf Proc IEEE Eng Med Biol Soc* 2006; **1**: 4326-8.
15. Reid B, Nuccitelli R, Zhao M. Non-invasive measurement of bioelectric currents with a vibrating probe. *Nat Protoc* 2007; **2**(3): 661-9.
16. Nuccitelli R, Nuccitelli P, Ramlatchan S, Sanger R, Smith P. Imaging the electric field associated with mouse and human skin wounds. *Wound Repair Regen* 2008; **16**: 432-41.
17. Zhao M, Song B, Pu J, Wada T, Reid B, Tai G, Wang F, Guo A, Walczysko P, Gu Y, Sasaki T, Suzuki A, Forrester JV, Bourne HR, Devreotes PN, McCaig CD, Penninger JM. Electrical signals control wound healing through phosphatidylinositol-3-OH kinase-gamma and PTEN. *Nature* 2006; **442**(7101):457-60.
18. Zhao M. Electrical fields in wound healing-an overriding signal that directs cell migration. *Semin Cell Dev Biol* 2009; **20**(6): 674-82.
19. Ojngwa JC, Isseroff RR. Electrical stimulation of wound healing. *J Invest Dermatol* 2003; **121**: 1-12.
20. Farboud B, Nuccitelli R, Schwab IR, Isseroff RR. DC electric fields induce rapid directional migration in cultured human corneal epithelial cells. *Exp Eye Res* 2000; **70**: 667-73.
21. Soong HK, Parkinson WC, Bafna S, Sulik GL, Huang SC. Movements of cultured corneal epithelial cells and stromal fibroblasts in electric fields. *Invest Ophthalmol Vis Sci* 1990; **31**(11): 2278-82.
22. Zhao M, McCaig CD, Agius-Fernandez A, Forrester JV, Araki-Sasaki K. Human corneal epithelial cells reorient and migrate cathodally in a small applied electric field. *Curr Eye Res* **1997**; **16**: 973-84.
23. Zhao M, Agius-Fernandez A, Forrester JV, McCaig CD. Directed migration of corneal epithelial sheets in physiological electric fields. *Invest Ophthalmol Vis Sci* 1996; **37**(13): 2548-58.
24. Nishimura KY, Isseroff RR, Nuccitelli R. Human keratinocytes migrate to the negative pole in direct current electric fields comparable to those measured in mammalian wounds. *J Cell Sci* 1996; **109**: 199-207.
25. Fang KS, Farboud B, Nuccitelli R, Isseroff RR. Migration of human keratinocytes in electric fields requires growth factors and extracellular calcium. *J Invest Dermatol* 1998; **111**:751-6.
26. Robinson KR. The responses of cells to electric fields: a review. *J Cell Biol* 1985; **101**(6): 2023-7.

27. Hinkle L, McCaig CD, Robinson KR. The direction of growth of differentiating neurons and myoblasts from frog embryos in an applied electric field. *J Physiol (Lond)* 1981; **314**: 121-35.
28. Patel N, Poo MM. Orientation of neurite growth by extracellular electric fields. *J Neurosci* 1982; **2**: 483-96.
29. Stump RF, Robinson KR. Xenopus neural crest cell migration in an applied electrical field. *J Cell Biol* 1983; **97**: 1226-33.
30. Vieira AC, Reid B, Cao L, Mannis MJ, Schwab IR, Zhao M. Ionic components of electric current at rat corneal wounds. *PLoS One* 2011; **6(2)**:e17411.
31. Nuccitelli R. A role for endogenous electric fields in wound healing. *Curr Top Dev Biol* 2003; **58**: 1-26.
32. Nuccitelli R. Physiologic electric fields can influence cell motility, growth, and polarity. *Adv Cell Biol* 1988; **2**:213-33.
33. McCaig CD, Zhao M. Physiological electrical fields modify cell behaviour. *Bioessays* 1997; **19**: 819-26.
34. Foulds IS, Barker AT. Human skin battery potentials and their possible role in wound healing. *Br J Dermatol* 1983; **109**: 515-22.
35. Zhao M, Song B, Pu J, et al. Electrical signals control wound healing through phosphatidylinositol-3-OH kinase-gamma and PTEN. *Nature* 2006; **442(7101)**: 457-60.
36. Zhao M, Forrester JV, McCaig CD. A small, physiological electric field orients cell division. *Proc Natl Acad Sci USA* 1999; **96**: 4942-6.
37. Sta Iglesia DD, Venable JW. Endogenous lateral electric fields around bovine corneal lesions are necessary for and can enhance normal rates of wound healing. *Wound Repair Regen* 1998; **6**: 531-42.
38. Messerli MA, Graham DM. Extracellular electrical fields direct wound healing and regeneration. *Biol Bull* 2011; **221**: 79-92.
39. Piccolino M. Animal electricity and the birth of electrophysiology: the legacy of Luigi Galvani. *Brain Research Bulletin* 1998; **46**: 381-407.
40. McCaig CD, Rajnicek AM, Song B, Zhao M. Controlling cell behavior electrically: current views and future potential. *Physiol Rev* 2005; **85**: 943-78.
41. Zadunaisky JA. Active transport of chloride in frog cornea. *Am J Phys* 1966; **211**:505-12.
42. Zadunaisky JA, Lande MA. Active chloride transport and control of corneal transparency. *Am J Phys* 1971; **221**: 1837-44.
43. Yue J, Zhang Q, Sun Z, Du W, Yu C. A case of electroacupuncture therapy for pressure ulcer. *Acupunct Med* 2013;**31(4)**:450-1
44. Zhang QH, Yue JH, Sun ZR. Electroacupuncture for pressure ulcer: a study protocol for a randomized controlled pilot trial. *Trials* 2014;**15**:7.
45. Zhang QH, Sun ZR, Yue JH, Ren X, Qiu LB, Lv XL, Du W. Traditional Chinese medicine for pressure ulcer: a meta-analysis. *Int Wound J* 2013;**10(2)**:221-31.
46. Zhang Q, Yue J, Sun Z. Massage therapy for preventing pressure ulcers. *Cochrane Database of Systematic Reviews* 2013 , Issue 5 . Art. No.: CD010518. DOI: 10.1002/14651858.CD010518 .